Networks and Heterogeneous Media

http://www.aimspress.com/journal/nhm

NHM, 20(3): 970–986.
DOI: 10.3934/nhm.2025042
Received: 11 July 2025
Revised: 30 August 2025
Accepted: 09 September 2025
Published: 15 September 2025

Research article

Error analysis of a finite difference scheme on a modified graded mesh for a nonlocal-in-time parabolic equation

Shujun Liu[1], **Li-Bin Liu**[1,*] **and Xiaobing Bao**[2]

[1] Center for Applied Mathematics of Guangxi, Nanning Normal University, Nanning 530100, China

[2] School of Big Data and Artificial Intelligence Chizhou University Chizhou, Anhui 247000, China

* **Correspondence:** Email: liulibin969@163.com.

Abstract: In this paper, a novel numerical method is developed to solve a parabolic diffusion equation with a nonlocal-in-time operator. First, drawing upon the mesh equidistribution principle, a modified graded mesh along with its properties is introduced. Additionally, the spatial derivative is discretized using the standard central difference scheme on a uniform mesh, whereas the time nonlocal operator is approximated by employing a finite difference scheme on the aforementioned modified graded mesh. Furthermore, the stability and convergence of our proposed scheme are demonstrated. Finally, the theoretical findings are corroborated through a series of numerical experiments.

Keywords: nonlocal-in-time operator; parabolic diffusion equation; finite difference scheme; modified graded mesh

1. Introduction

In this paper, we consider the following parabolic problem with a nonlocal-in-time operator:

$$\begin{cases} G_\delta u(x,t) - \frac{\partial^2 u(x,t)}{\partial x^2} = f(x,t), & \text{in } \Omega \times [0,T], \\ u(0,t) = u(1,t) = 0, & \text{in } \partial\Omega \times [0,T], \\ u(x,t) = g(x,t), & \text{in } \Omega \times (-\delta, 0), \end{cases} \tag{1.1}$$

where $\Omega = (0,1)$, δ is a nonlocal horizon parameter, and g, f are two known functions. Here, for the given fractional kernel function $\rho_\delta(s)$, the nonlocal-in-time operator G_δ is defined by following:

$$G_\delta u(t) = \int_0^\delta (u(t) - u(t-s)) s \rho_\delta(s)\, ds,$$

where we assume that the non-negative kernel $\rho_\delta(s)$ has a compact support contained in the interval $[0, \delta]$ and satisfies a normalized second moment

$$\int_0^\delta s^2 \rho_\delta(s) ds = 1. \tag{1.2}$$

Under these assumptions, Eq (1.1) has a unique weak solution (see Theorem 4.1 of [1]).

Nonlocal models, which include interactions or dependencies that extend beyond immediate spatial or temporal neighborhoods to provide more accurate descriptions of complex systems, are widely used across scientific disciplines in social sciences [2], physics [3], materials science [4–6], and biology and life science [7]. It is noteworthy that nonlocal models, which have garnered increasing attention in various scientific and engineering fields in recent years, encompass both spatial nonlocal and temporal nonlocal models. Spatial nonlocal models take the interactions between different spatial locations that extend beyond the immediate neighborhood into account, meaning that the state or behavior at a particular point in space is influenced not only by its local surroundings but also by distant regions [8]. On the other hand, temporal nonlocal models focus on the nonlocal dependencies in time. It is well known that the nonlocal-in-time equation provides a more generalized form of classical and fractional diffusion equations. Most notably, remarkable progress has been made in the study of fractional time-diffusion equations [9, 10]. Consequently, it's crucial to obtain numerical solutions for nonlocal models that encompass spatial and temporal nonlocal types. They enable us to verify theoretical assumptions, solve complex real-world problems in engineering and biomedicine, and explore new phenomena that local models can't reveal.

In recent years, the development of numerical methods for nonlocal-in-space problems has garnered significant and widespread interest within the academic and research communities [11]. For instance, the authors of [12] explored various numerical approaches, specifically the finite difference finite element methods, to solve nonlocal diffusion and linear peridynamic equations. In a more recent study, Mezzanotte et al. [13] presented an innovative combination of finite differences and generalized Bernstein polynomials. Simultaneously, Li and Fu [14] made a notable contribution by constructing a linear implicit energy-conserving scheme for nonlocal wave equations. They achieved this through the application of the generalized scalar auxiliary variable (GSAV) method, which offers a promising approach to accurately simulate wave propagation in nonlocal systems while preserving energy conservation. In [15], another significant advancement was made with the formulation of a nonlocal diffusion model for bond bases with matrix coefficients. This model was characterized by a linear configurational discretization scheme that ingeniously utilized Gaussian kernel functions, which enabled more efficient and accurate numerical simulations of nonlocal diffusion processes. Moreover, the authors in [16] proposed a fast and efficient algorithm that ingeniously combined Proper Orthogonal Decomposition (POD) with local Radial Basis Function (RBF) collocation.

It is noteworthy that methods specifically tailored for nonlocal-in-space problems cannot be straightforwardly applied to nonlocal-in-time problems. This is primarily due to the intrinsic temporal asymmetry and irreversibility that characterize nonlocal-in-time scenarios. Recognizing this limitation, researchers have been actively pursuing studies on nonlocal-in-time problems within asymmetric domains [17]. Chen et al. [18] adopted a uniform grid discretization and a quadrature-based finite difference method to construct a discrete nonlocal time operator. The temporal error convergence order of this method was first-order, and was achieved by transforming integrals

into node-valued weighted sums. The authors of [19] introduced a backward difference discretization for the temporal direction on a uniform grid. Analyses of the time operator and entropy method showed that, the entropy decay time and L^1 error converged with rates $O(t^{-\alpha})$ and $O(t^{-\alpha/2})$, respectively, for fractional-order time diffusion. Du et al. [20] constructed a continuous-time model via a nonlocal time operator that avoided traditional time-grid discretization. The operator, which was based on the integral of $\rho_\delta(s)$ over $(0, \delta)$, eliminated explicit time partitioning. Experiments validated the model's diffusion properties across temporal regimes. Additionally, the authors of [21] reviewed discrete methods for nonlocal time-kernel construction on uniform grids; they compared explicit central difference and Newmark implicit schemes for dynamical equations. The experiments showed that the implicit scheme matched the central difference accuracy while reducing computation time by over 20 times.

However, the asymmetry of nonlocal-in-time operators often induces weak endpoint singularities in solutions, which restricts the uniform mesh convergence to first order; additionally, non-uniform grids are typically employed to improve the convergence rates. However, the interaction between nonuniform meshes and boundary singularities in nonlocal-in-time operator discretization remains underexplored. Moreover, discretizing nonlocal memory models presents additional challenges: the nonlocal horizon parameter δ and integral kernel functions may position solution points off mesh nodes, which complicates the equation approximation. The scarcity of research on nonlocal-in-time problems further highlights the need for efficient numerical methods to overcome these obstacles.

In this work, based on the existing convergence results for the graded mesh and the optimal graded index, and inspired by reference [22], we propose an improved version of the graded mesh to ensure that the modified mesh produces less computational error than the graded mesh with the same order of convergence.

The structure of this paper is as follows: In Section 2, we collect some conclusions that are necessary for the proof process; in Section 3, we present a modified form of the graded mesh and analyze some properties of this modified mesh; in Section 4, we present the discretization scheme for non-uniform meshes and discuss the stability of the scheme; in Sections 5, we evaluate the error estimates and the corresponding convergence of the scheme; in Section 6, we verify the theoretical results presented in the article using a numerical example; and some concluding discussions are provided in Section 7.

Notation: In this article, M and N represent two positive integer grid parameters. C denotes a positive constant that is independent of α, M, and N; additionally, it can take on different values in various contexts.

2. Preliminary results

In this section, we collect some preliminary results that will be used in the following sections. Specifically, we explain how the regularity of the weak solution $u(x,t)$ depends on the regularity of the initial data $g(x,t)$. We let $\rho_\delta(s) = (\alpha+1)s^{\alpha-2}\delta^{-1-\alpha}$, with $\alpha \in (0,1)$. The following lemma is an extension of Theorem 4.1 in the reference [1]; the proof process is omitted here.

Lemma 2.1 ([1],Theorem 4.1)**.** *Let $g(x,t) = \phi(x)\varphi(t) \in L^\infty(-\delta, 0; H^\alpha(\Omega))$, with $\alpha \in (0,1)$ and $f \equiv 0$. When $t > 0$, problem* (1.1) *has a unique weak solution $u(x,t)$ that satisfies the following:*

$$\|u(x,t)\|_{H^{\alpha+2}(\Omega)} \le Ct\|g\|_{L^\infty(-\delta,0;H^\alpha(\Omega))}.$$

According to Theorem 4.1 and Remark 4.1 in [1], we know that $g(x,t) = \phi(x)\varphi(t) \in L^\infty(-\delta, 0; H^\alpha(\Omega))$ for variables-separable initial data, with $\alpha \in (0,1)$ and $f \equiv 0$. We assume that $g(x,t)$ satisfies $|g(x,t)| \leq C\,|t|^\alpha$ for $t \in (-\delta, 0)$; then, there exists a unique weak solution $u(x,t)$ to Eq (1.1) which satisfies the following regularity estimation bounds.

The regularity of the weak solution $u(x,t)$ for $t \in (0,\epsilon], \epsilon \to 0^+$ aligns with the regularity of the initial condition $g(x,t)$ in the Hilbert space. Additionally, for $t > \epsilon$, the regularity of $u(x,t)$ increases to $H^{\alpha+2}$ as time advances. Additionally, this shows that the smoothness of the solution improves due to the effect of the kernel $\rho_\delta(s)$. Furthermore, we can make the following reasonable assumptions. Then, one has the following lemma.

Lemma 2.2. *Let $g(x,t) = \phi(x)\varphi(t) \in L^\infty(-\delta, 0; H^\alpha(\Omega))$, with $\alpha \in (0,1)$. When the weak solution $u(x,t) \in H^\alpha$ for $t \in (0,\epsilon]$, with $\epsilon \to 0^+$, we have the following:*

$$\left|\frac{\partial^k u}{\partial t^k}(x,t)\right| \leq Ct^{\alpha-k},\ k = 1,2,3. \tag{2.1}$$

Furthermore, when the weak solution $u(x,t) \in H^{\alpha+2}$ for $t > \epsilon$, one has the following:

$$\left|\frac{\partial^k u}{\partial t^k}(x,t)\right| \leq Ct^{\alpha+2-k},\ k = 1,2,3. \tag{2.2}$$

3. A modified graded mesh

Let $\bar{\Omega}_t^N := \{0 = t_0 < t_1 < \cdots < t_N = T\}$ be an arbitrary non-uniform grid with the local mesh size $\tau_{k+1} = t_{k+1} - t_k$. Set $\tau = \max\{\tau_{k+1}\}_{k=0}^{N-1}$ and denote $I_k = (t_k, t_{k+1})$ for $0 \leq k \leq N-1$. Next, to obtain the specific mesh nodes $\{t_k\}_{k=0}^N$, we choose the mesh monitor function

$$\tilde{M}(\cdot,t) = \max\left\{T, Kt^{\frac{1}{\gamma}-1}\right\}$$

to ensure that grid nodes $\{t_k\}_{k=0}^N$ satisfy the following equation:

$$\int_{t_k}^{t_{k+1}} \tilde{M}(\cdot,s)\,ds = \frac{1}{N}\int_0^T \tilde{M}(\cdot,s)\,ds, \tag{3.1}$$

where $K \in (0,T)$ is a user-chosen constant, and $\gamma > 1$ is a parameter related to the regularity of the function. Furthermore, let $\sigma = (\frac{T}{K})^{\frac{\gamma}{1-\gamma}}$; there exist a sub-interval $I := [\sigma, T]$ and an index J such that

$$0 < Kt^{\frac{1}{\gamma}-1} \leq T,\ \ \forall t \in I,\ \ t_{J-1} < \sigma \leq t_J.$$

By simple calculation, we obtain the following:

$$t_k = \begin{cases} \left(\frac{\alpha P}{2K}\right)^\gamma \left(\frac{k}{N}\right)^\gamma, & k = 0,1,\cdots,J-1, \\ (1-\frac{2}{\alpha})\sigma + \frac{Pk}{TN}, & k = J, J+1,\cdots,N, \end{cases} \tag{3.2}$$

where $P = \int_0^T \tilde{M}(\cdot,s)\,ds = (\gamma-1)T\sigma + T^2$. Obviously, for $T \geq 1$, we have $P/T > 1$.

Lemma 3.1. *Let* $\{t_k\}_{k=0}^{N}$ *denote the modified graded mesh defined in Eq* (3.2)*. Then, we have the following:*

$$t_k \leq \begin{cases} Ck^{\gamma}N^{-\gamma}, & k = 0, 1, \cdots, J-1, \\ CN^{-1}, & k = J, J+1, \cdots, N, \end{cases} \tag{3.3}$$

$$\tau_k \leq CN^{-1}, \quad k = 0, 1, \cdots, N. \tag{3.4}$$

Proof. For $k = 0, 1, \cdots, J-1$, where the point $\{t_k\}_{k=0}^{J-1}$ is the graded grid, then we have the following:

$$t_k = \left(\frac{\alpha P}{2K}\right)^{\gamma}\left(\frac{k}{N}\right)^{\gamma} \leq Ck^{\gamma}N^{-\gamma}.$$

For $k = J, J+1, \cdots, N$, where the point $\{t_k\}_{k=J}^{N}$ is the uniform grid, then we have the following:

$$t_k = \left(1 - \frac{2}{\alpha}\right)\sigma + \frac{Pk}{TN} \leq \frac{Pk}{TN} \leq CN^{-1}.$$

Finally, for $k = 1, \cdots, N$, it follows from Eqs (3.1) and (3.2) that

$$\tau_k = \frac{1}{T}\int_{t_{k-1}}^{t_k} T dt \leq \frac{1}{T}\int_{t_{k-1}}^{t_k} \tilde{M}(\cdot, t)dt = \frac{1}{MT}\int_0^T \tilde{M}(\cdot, t)dt = \frac{P}{MT} \leq CN^{-1}.$$

Thus, the proof is completed.

Lemma 3.2. *Let* $\{t_k\}_{k=1}^{N}$ *be the modified graded mesh defined in Eq* (3.2)*, and* $u(x,t)$ *be the exact solution to Eq (1.1). For* $k = 1, \cdots, N$*, we set* $m \leq k-1$ *and let* $\gamma = \frac{2}{\alpha}$*, with* $x \in [0,1]$*. Then, it follows that*

$$\int_{t_m}^{t_{m+1}} \left|\frac{\partial^2 u}{\partial \mu^2}(x, t_k - \mu)\mu\right| d\mu \leq CN^{-2}. \tag{3.5}$$

Proof. From Eqs (3.1) and (3.2) and invoking Lemma 3.1, one has the following:

$$\begin{aligned} \int_{t_m}^{t_{m+1}} \left|\frac{\partial^2 u}{\partial \mu^2}(x, t_k - \mu)\mu\right| d\mu &\leq C\int_{t_m}^{t_{m+1}} \left|(t_k - \mu)^{\alpha-2}\mu\right| d\mu \\ &= C\int_{t_k - t_{m+1}}^{t_k - t_m} \left|\mu^{\alpha-2}(\mu - t_k)\right| d\mu \\ &\leq C\int_{t_k}^{t_{k+1}} \mu^{\alpha-2}(\mu - t_k)d\mu \\ &\leq C\left(\int_{t_k}^{t_{k+1}} \mu^{\frac{\alpha}{2}-1}d\mu\right)^2 \\ &\leq C\left(\int_{t_k}^{t_{k+1}} \tilde{M}(\cdot, \mu)d\mu\right)^2 \\ &\leq CN^{-2}, \end{aligned}$$

where

$$\int_a^b \phi(t)(t-a)dt \leq \frac{1}{2}\left(\int_a^b \sqrt{\phi(t)}dt\right)^2.$$

This conclusion applies to any positive, monotonically decreasing function $\phi(t)$ over the interval $[a, b]$ [22]. This completes the proof.

4. The discrete scheme

Let M be a positive integer, and $\bar{\Omega}_x^M := \{0 = x_0 < x_1 < \cdots < x_M = 1\}$ be a spatial uniform mesh with $h = \frac{1}{M}$. For the time mesh, we use the modified graded mesh defined in Eq (3.2). Considering the nonlocal constant δ, we assume that $\delta = t_{r_t} + \delta_0$ for a nonnegative integer $r_t < N$ and $\delta_0 \in [0, \tau_{r_t+1}]$. Particularly, if $\delta_0 \neq 0$, then we denote $I_{r_t} = [t_{r_t}, \delta]$.

Let U_i^k be the numerical approximation of the solution $u(x,t)$ at the discrete nodal points $Q^{M,N} = \{(x_i, t_k), i = 0, 1, \cdots, M, k = 0, 1, \cdots, N\}$. Then, for $k = 1, 2, \cdots, N$, we define the spatial difference operator δ_x^2 and temporal approximation operator $G_{M,N}^{\alpha}$ as follows:

$$\begin{aligned} \delta_x^2 U_i^k &= \frac{U_{i+1}^k - 2U_i^k + U_{i-1}^k}{h^2}, \\ G_{M,N}^{\alpha} U_i^k &:= \sum_{m=1}^{r_t-1} \frac{U_i^k - U_i^{k-m}}{t_m} \int_{I_m} s^2 \rho_\delta(s) ds + \frac{U_i^k - U_i^{k-r_t}}{t_{r_t}} \int_{I_{r_t}} s^2 \rho_\delta(s) ds \\ &= C_{\alpha\delta} \sum_{m=1}^{r_t-1} \frac{U_i^k - U_i^{k-m}}{t_m} \int_{I_m} s^{\alpha} ds + C_{\alpha\delta} \frac{U_i^k - U_i^{k-r_t}}{t_{r_t}} \int_{I_{r_t}} s^{\alpha} ds, \end{aligned} \tag{4.1}$$

where $C_{\alpha\delta} = \frac{1+\alpha}{\delta^{1+\alpha}}$ is a constant dependent on α and the nonlocal horizon parameter δ. Thus, for $m = 1, 2, \cdots, r_t$, $i = 1, 2, \cdots, M-1$, and $k = 1, 2, \cdots, N$, the discretization scheme of Eq (1.1) can be given by the following:

$$\begin{cases} L_{M,N} U_i^k := G_{M,N}^{\alpha} U_i^k - \delta_x^2 U_i^k = f(x_i, t_k), \\ U_0^k = 0,\ U_M^k = 0, \\ U_i^{k-m} = g(x_i, t_k - t_m),\ t_k < t_m. \end{cases} \tag{4.2}$$

Remark 4.1. *It should be noted that $t_k - t_m$ may not equal a specific node t_j. Therefore, for practical calculations, we will use the linear interpolation technique to obtain the value of U_i^{k-m}.*

Denote the following:

$$\begin{aligned} &\omega_m = \int_{I_m} s^{\alpha} ds,\ m = 1, 2, \cdots, r_t, \\ &\mathbf{U}^k = (U_0^k, U_1^k, \cdots, U_M^k)^T, \\ &\mathbf{f}^k = (f(x_0, t_k), f(x_1, t_k), \cdots, f(x_M, t_k))^T, \\ &\mathbf{g}(t) = (g(x_0, t), g(x_1, t), \cdots, g(x_M, t))^T. \end{aligned}$$

Then, the following theorem lists the stability result of the discretization scheme within Eq (4.2).

Theorem 4.1. *Let $b_{\alpha\delta} = C_{\alpha\delta} \sum_{m=1}^{r_t} \frac{\omega_m}{t_m}$. Then, the solution $\mathbf{U}^k$ of the discretization scheme within Eq* (4.2) *satisfies the following:*

$$\|\mathbf{U}^k\|_\infty \leq C \left(\|\mathbf{g}(t)\|_\infty + \frac{1}{b_{\alpha\delta}} \max_{1 \leq j \leq k} \|\mathbf{f}^j\|_\infty \right), \quad k = 1, \cdots, N. \tag{4.3}$$

Proof. We prove this theorem using mathematical induction for $k \in \{1, 2, \cdots, N\}$.

Choose m_0 such that $\left|U^k_{m_0}\right| = \|\mathbf{U}^k\|_\infty$. We start with the case $m_0 \in \mathbb{Z} \setminus \{0\}$, when $k = 1$; the discretization scheme (4.2) at the grid points (x_{m_0}, t_1) can be written as follows:

$$C_{\alpha\delta}\sum_{m=1}^{r_t}\frac{\omega_m}{t_m}U^1_{m_0} + \frac{2U^1_{m_0}}{h^2} = \frac{U^1_{m_0+1} + U^1_{m_0-1}}{h^2} + C_{\alpha\delta}\sum_{m=1}^{r_t}\frac{\omega_m}{t_m}U^{1-m}_{m_0} + f^1_{m_0}. \tag{4.4}$$

Note that $b_{\alpha\delta} > 0$ and is bounded. Then, based on Eq (4.4), one has the following:

$$\left|U^1_{m_0}\right| \leq \frac{1}{b_{\alpha\delta}+\frac{2}{h^2}}\left|C_{\alpha\delta}\sum_{m=1}^{r_t}\frac{\omega_m}{t_m}U^{1-m}_{m_0} + f^1_{m_0}\right| + \frac{\frac{2}{h^2}}{b_{\alpha\delta}+\frac{2}{h^2}}\left|U^1_{m_0}\right|. \tag{4.5}$$

This yields the following:,

$$\begin{aligned}\left|U^1_{m_0}\right| &\leq \left\|g(x_{m_0}, t)\right\|_\infty + \frac{1}{b_{\alpha\delta}}\left|f^1_{m_0}\right| \\ &\leq \|\mathbf{g}(t)\|_\infty + \frac{1}{b_{\alpha\delta}}\left\|\mathbf{f}^1\right\|_\infty.\end{aligned}$$

Suppose that for $k = 1, 2, \cdots, N-1$, one has the following:

$$\left|U^k_{m_0}\right| \leq \|\mathbf{g}(t)\|_\infty + \frac{1}{b_{\alpha\delta}}\max_{1\leq j\leq k}\left\|\mathbf{f}^j\right\|_\infty.$$

Then, for $k = N$, we obtain the following:

$$\begin{aligned}\left|U^N_{m_0}\right| &\leq \frac{1}{b_{\alpha\delta}}\left|C_{\alpha\delta}\sum_{m=1}^{r_t}\frac{\omega_m}{t_m}U^{N-m}_{m_0} + f^N_{m_0}\right| \\ &\leq \frac{1}{b_{\alpha\delta}}\left|C_{\alpha\delta}\sum_{m=1}^{r_t}\frac{\omega_m}{t_m}\left[\|\mathbf{g}(t)\|_\infty + \frac{1}{b_{\alpha\delta}}\max_{1\leq j\leq k}\left\|\mathbf{f}^j\right\|_\infty\right] + f^N_{m_0}\right| \\ &\leq \|\mathbf{g}(t)\|_\infty + \frac{1}{b_{\alpha\delta}}\max_{1\leq j\leq N}\left\|\mathbf{f}^j\right\|_\infty.\end{aligned}$$

Next, we discuss the case when $m_0 = 0$. It follows from Eq (4.2) that

$$\left(b_{\alpha\delta} + \frac{1}{h^2}\right)U^k_0 = \frac{U^k_2 - 2U^k_1}{h^2} + C_{\alpha\delta}\sum_{m=1}^{r_t}\frac{\omega_m}{t_m}U^{k-m}_0 + f^k_0. \tag{4.6}$$

For the above result, when $f \equiv 0$, it is clear to observe that $|U^k_{m_0}| \leq C\|\mathbf{g}(t)\|_\infty$ for all $1 \leq k \leq N$ using the preceding argument. Therefore, it suffices to consider the case when $g \equiv 0$. By mathematical

induction and Eq (4.4), invoking Eq (4.2), we can prove the following:

$$\begin{aligned}
\left(b_{\alpha\delta}+\frac{1}{h^2}\right)\left|U_0^k\right| &\le \frac{1}{h^2}\left|U_0^k\right| + C_{\alpha\delta}\sum_{m=1}^{r_t}\frac{\omega_m}{t_m}\left|U_0^{k-m}\right| + \left|f_0^k\right| \\
\left|U_0^k\right| &\le \frac{1}{b_{\alpha\delta}}\left(C_{\alpha\delta}\sum_{m=1}^{k-1}\frac{\omega_m}{t_m}\left|U_0^{k-m}\right| + C_{\alpha\delta}\sum_{m=k}^{r_t}\frac{\omega_m}{t_m}\left|U_0^{k-m}\right| + \left|f_0^k\right|\right) \\
&\le \frac{1}{b_{\alpha\delta}}\left(C_{\alpha\delta}\sum_{m=1}^{k-1}\frac{\omega_m}{t_m}\left|U_0^{k-m}\right| + \left|f_0^k\right|\right) \\
&\le \frac{1}{b_{\alpha\delta}}\left(C_{\alpha\delta}\sum_{m=1}^{k-1}\frac{\omega_m}{t_m}\left|\|\mathbf{g}(t)\|_\infty + \frac{1}{b_{\alpha\delta}}\max_{1\le j\le k-m}\left\|\mathbf{f}^j\right\|_\infty\right| + \left|f_0^k\right|\right) \\
&\le C\frac{1}{b_{\alpha\delta}}\max_{1\le j\le k}\left\|\mathbf{f}^j\right\|_\infty .
\end{aligned}$$

Through the above analysis, the proof is complete.

5. Truncation error and convergence for scheme

5.1. Truncation error for the time discrete scheme

For a given index $i(1 \le i \le M-1)$ and $k = 1, 2, \cdots, N$, the truncation error for the nonlocal-in-time discrete operator can be given as follows:

$$R_i^k = G_{M,N}^{\alpha}u(x_i,t_k) - G_\delta u(x_i,t_k) = \sum_{m=1}^{r_t-1}T_{km} + T_{kr_t},$$

where

$$\begin{aligned}
T_{km} &:= C_{\alpha\delta}\int_{s=t_m}^{t_{m+1}} s^{\alpha}\left[\frac{u(x_i,t_k)-u(x_i,t_k-t_m)}{t_m} - \frac{u(x_i,t_k)-u(x_i,t_k-s)}{s}\right]ds, \\
T_{kr_t} &:= C_{\alpha\delta}\int_{s=t_{r_t}}^{\delta} s^{\alpha}\left[\frac{u(x_i,t_k)-u(x_i,t_k-t_m)}{t_m} - \frac{u(x_i,t_k)-u(x_i,t_k-s)}{s}\right]ds.
\end{aligned} \tag{5.1}$$

For $\delta_0 \in (0, \tau_{r_t+1})$, it is easy to show that

$$\left|R_i^k\right| \le \sum_{m=1}^{r_t}|T_{km}| .$$

Lemma 5.1. *For $i = 1, 2, \cdots, M-1$, $k = 1, 2, \cdots, N$, we have the following:*

$$|T_{k,m}| \le \begin{cases} C\int_{t_m}^{t_{m+1}} s^{\alpha-1}ds\int_{t_m}^{t_{m+1}}\left|\frac{\partial^2 u}{\partial\mu^2}(x_i,t_k-\mu)\mu\right|d\mu, & 0\le m\le k-1, \\ C\left[\int_{t_m}^{t_{m+1}} s^{\alpha-1}(s-t_m)ds + \int_{t_m}^{t_{m+1}} s^{\alpha-1}ds\int_{t_m}^{t_{m+1}}\left|\frac{\partial^2 g}{\partial\mu^2}(x_i,t_k-\mu)\mu\right|d\mu\right], & k\le m\le r_t. \end{cases} \tag{5.2}$$

Proof. First, let $\phi(\zeta) = \int_{t_k-\zeta}^{t_k} \frac{\partial^2 u}{\partial \mu^2}(x_i,\mu)(t_k-\mu)d\mu$; then, one has the following:

$$\begin{aligned}\left|\int_{t_m}^{t_{m+1}} s^{\alpha-1}\phi(s)ds\right| &= \left|\int_{t_m}^{t_{m+1}} s^{\alpha-1}\int_{t_k-s}^{t_k}\frac{\partial^2 u}{\partial \mu^2}(x_i,\mu)(t_k-\mu)d\mu ds\right| \\ &= \left|\int_{t_k-t_{m+1}}^{t_k-t_m}\frac{\partial^2 u}{\partial \mu^2}(x_i,\mu)(t_k-\mu)\int_{t_k-\mu}^{t_{m+1}} s^{\alpha-1}ds d\mu\right| \\ &= \left|\int_{t_m}^{t_{m+1}}\frac{\partial^2 u}{\partial \mu^2}(x_i,t_k-\mu)\mu\int_{\mu}^{t_{m+1}} s^{\alpha-1}ds d\mu\right| \\ &\le C\int_{t_m}^{t_{m+1}} s^{\alpha-1}ds\int_{t_m}^{t_{m+1}}\left|\frac{\partial^2 u}{\partial \mu^2}(x_i,t_k-\mu)\mu\right|d\mu.\end{aligned}$$

Similarly, by the additivity of the integral interval, we can obtain the following:

$$\begin{aligned}\left|\frac{1}{t_m}\int_{t_m}^{t_{m+1}} s^{\alpha}\phi(t_m)ds\right| &= \left|\frac{1}{t_m}\int_{t_m}^{t_{m+1}} s^{\alpha}ds\int_{t_k-t_m}^{t_k}\frac{\partial^2 u}{\partial \mu^2}(x_i,\mu)(t_k-\mu)d\mu\right| \\ &\le C\frac{t_{m+1}}{t_m}\int_{t_m}^{t_{m+1}} s^{\alpha-1}ds\int_{t_k-t_m}^{t_k}\left|\frac{\partial^2 u}{\partial \mu^2}(x_i,\mu)(t_k-\mu)\right|d\mu \\ &\le C\int_{t_m}^{t_{m+1}} s^{\alpha-1}ds\int_{t_m}^{t_{m+1}}\left|\frac{\partial^2 u}{\partial \mu^2}(x_i,t_k-\mu)\mu\right|d\mu.\end{aligned}$$

Then, for $0 \le m \le k-1$, using the Taylor expansion with an integral remainder term, we have the following:

$$\begin{aligned}|T_{km}| &= C_{\alpha\delta}\left|\int_{t_m}^{t_{m+1}} s^{\alpha}\left[\frac{1}{s}\phi(s)-\frac{1}{t_m}\phi(t_m)\right]ds\right| \\ &\le C_{\alpha\delta}\left|\int_{t_m}^{t_{m+1}} s^{\alpha-1}\phi(s)ds\right| + C_{\alpha\delta}\left|\frac{1}{t_m}\int_{t_m}^{t_{m+1}} s^{\alpha}\phi(t_m)ds\right| \\ &\le C\int_{t_m}^{t_{m+1}} s^{\alpha-1}ds\int_{t_m}^{t_{m+1}}\left|\frac{\partial^2 u}{\partial \mu^2}(x_i,t_k-\mu)\mu\right|d\mu.\end{aligned}$$

Next, for $k \le m \le r_t$ and $k > 0$,

$$\begin{aligned}|T_{km}| &\le C_{\alpha\delta}\left|\int_{t_m}^{t_{m+1}} s^{\alpha}\left[\frac{u(x_i,t_k)-g(x_i,t_k-t_m)}{t_m}-\frac{u(x_i,t_k)-g(x_i,t_k-s)}{s}\right]ds\right| \\ &\le C_{\alpha\delta}\left[\frac{|u(x_i,t_k)|}{t_m}\int_{t_m}^{t_{m+1}} s^{\alpha-1}(s-t_m)ds+\int_{t_m}^{t_{m+1}} s^{\alpha}\left|\frac{g(x_i,t_k-s)}{s}-\frac{g(x_i,t_k-t_m)}{t_m}\right|ds\right].\end{aligned}$$

For the first item, invoking Lemma 2.1, we have the following:

$$\begin{aligned}\frac{|u(x_i,t_k)|}{t_m}\int_{t_m}^{t_{m+1}} s^{\alpha-1}(s-t_m)ds &\le C\left|t_k\|g\|_{L^\infty(-\delta,0;H^\alpha(\Omega))}\right|\frac{1}{t_m}\int_{t_m}^{t_{m+1}} s^{\alpha-1}(s-t_m)ds \\ &\le C\frac{t_k^{1+\alpha}}{t_m}\int_{t_m}^{t_{m+1}} s^{\alpha-1}(s-t_m)ds \\ &\le Cm^{\alpha}N^{-\alpha}\int_{t_m}^{t_{m+1}} s^{\alpha-1}(s-t_m)ds \\ &\le C\int_{t_m}^{t_{m+1}} s^{\alpha-1}(s-t_m)ds.\end{aligned}$$

For the second integral item, the proof process is the same as in the previous case and will be omitted here. Last, we achieve the desired result.

Lemma 5.2. *Under the modified graded mesh* $\{t_k\}_{k=1}^N$ *defined in Eq (3.2), one has the following:*

$$\left|R_n^k\right| \leq CN^{-(1+\alpha)}, k = 1, 2, \cdots, N.$$

Proof. Invoking Lemma 5.1, we divide our proof into the following three cases:

1. When $m = 0$, we discuss the estimations of $|T_{k,0}|(1 \leq k \leq N)$.
2. When $1 \leq m < r_t + 1$ and $m \leq k - 1$, we derive the estimations of $\sum_{m=1}^{J-1} |T_{k,m}|(1 \leq m < J)$, $\sum_{m=J}^{r_t} |T_{k,m}|(J \leq m < k - 1)$, and $|T_{k,m}|(m = k - 1)$.
3. When $1 \leq m < r_t + 1$ and $m \geq k$, we show the bounds of $\sum_{m=1}^{r_t-1} |T_{km}| (2 \leq r_t < N)$.

Case 1. For $m = 0$ and $1 \leq k \leq N$, it follows from Eqs (3.3) and (3.4) that it is easy to obtain the following:

$$\begin{aligned}
|T_{k,0}| &\leq C \int_{t_0}^{t_1} s^{\alpha-1} ds \int_{t_0}^{t_1} \left| \frac{\partial^2 u}{\partial \mu^2}(x_i, t_k - \mu)\mu \right| d\mu \\
&\leq CN^{-2} \left| \int_{t_0}^{t_1} s^{\alpha-1} ds \right| \\
&\leq CN^{-2}(t_1^\alpha - t_0^\alpha) \\
&\leq CN^{-2}N^{-\alpha} \\
&\leq CN^{-(2+\alpha)}.
\end{aligned}$$

Case 2. When $1 \leq m < r_t + 1$ and $m \leq k - 1$, using Eq (3.3), for $1 \leq m < J$, we have the following:

$$\begin{aligned}
\sum_{m=1}^{J-1} |T_{km}| &\leq C \sum_{m=1}^{J-1} \int_{t_m}^{t_{m+1}} s^{\alpha-1} ds \int_{t_m}^{t_{m+1}} \left| \frac{\partial^2 u}{\partial \mu^2}(x_i, t_k - \mu)\mu \right| d\mu \\
&\leq CN^{-2} \sum_{m=1}^{J-1} \int_{t_m}^{t_{m+1}} s^{\alpha-1} ds \\
&\leq CN^{-2}(t_J^\alpha - t_1^\alpha) \\
&\leq CN^{-2}N^{-\gamma\alpha} J^{\gamma\alpha} \\
&\leq CN^{-2}.
\end{aligned}$$

Furthermore, for $J \leq m < k - 1$, we have the following:

$$\begin{aligned}
\sum_{m=J}^{r_t} |T_{km}| &\leq C \sum_{m=J}^{r_t-1} \int_{t_m}^{t_{m+1}} s^{\alpha-1} ds \int_{t_m}^{t_{m+1}} \left| \frac{\partial^2 u}{\partial \mu^2}(x_i, t_k - \mu)\mu \right| d\mu \\
&\leq CN^{-2}(t_{r_t+1}^\alpha - t_J^\alpha) \\
&\leq CN^{-(2+\alpha)}.
\end{aligned}$$

For $m = k-1$, when $1 \le m < N$, we obtain the following:

$$\begin{aligned}|T_{k,m}| &\le C\int_{t_m}^{t_{m+1}} s^{\alpha-1}ds \int_{t_m}^{t_{m+1}} \left|\frac{\partial^2 u}{\partial \mu^2}(x_i, t_k-\mu)\mu\right| d\mu \\ &\le CN^{-2}\int_{t_{k-1}}^{t_k} s^{\alpha-1}ds \\ &\le CN^{-2}\left(t_k^\alpha - t_{k-1}^\alpha\right) \\ &\le CN^{-(2+\alpha)}.\end{aligned}$$

Case 3. For $1 \le m < r_t+1$, $m \ge k$, and $2 \le r_t < N$, it follows from Eq (5.2) that

$$\begin{aligned}\sum_{m=1}^{r_t-1}\left|T_{k,m}\right| &\le C\sum_{m=1}^{r_t-1}\left[\int_{t_m}^{t_{m+1}} s^{\alpha-1}(s-t_m)ds + \int_{t_m}^{t_{m+1}} s^{\alpha-1}ds\int_{t_m}^{t_{m+1}}\left|\frac{\partial^2 g}{\partial \mu^2}(x_i,t_k-\mu)\mu\right|d\mu\right] \\ &\le C\sum_{m=1}^{r_t-1}(t_{m+1}^\alpha - t_m^\alpha)\tau_{m+1} + CN^{-2}\sum_{m=1}^{r_t-1}(t_{m+1}^\alpha - t_m^\alpha) \\ &\le C\tau(t_{r_t}^\alpha - t_1^\alpha) + CN^{-2}(t_{r_t}^\alpha - t_1^\alpha) \\ &\le CN^{-1}N^{-\alpha} + CN^{-(2+\alpha)} \\ &\le CN^{-(1+\alpha)}.\end{aligned}$$

Ultimately, by combining the above, we achieve the desired result.

5.2. Convergence of the scheme

For $(x_i, t_k) \in Q^{M,N}$, it is easy to obtain the following truncation error estimation for the spatial derivative:

$$\widetilde{R}_i^k = \frac{\partial^2 u}{\partial x^2}(x_i,t_k) - \delta_x^2 U_i^k = O(h^2). \tag{5.3}$$

Let $e_i^k = U_i^k - u(x_i,t_k)$ be the truncation error of the numerical scheme Eq (4.2) at point (x_i,t_k). Then, for $m = 1,2,\cdots,r_t$, $i = 1,2,\cdots,M-1$, and $k = 1,2,\cdots,N$, we obtain the following error equation:

$$\begin{cases} L_{M,N}e_i^k := G_{M,N}^\alpha e_i^k - \delta_x^2 e_i^k = \widetilde{R}_i^k + R_i^k, \\ e_0^k = 0, e_M^k = 0, \\ e_i^{k-m} = 0, t_k < t_m. \end{cases} \tag{5.4}$$

Theorem 5.1. *There exists a constant C such that*

$$\max_{(x_i,t_k)\in Q^{M,N}}\left|U_i^k - u(x_i,t_k)\right| \le C(h^2 + N^{-(1+\alpha)}). \tag{5.5}$$

Proof. For $1 \le k \le N$, invoking the stability result from Theorem 4.1 and Lemma 5.2, for the mesh nodes $(x_i,t_k) \in Q^{M,N}$ we defined in Section 3, we yield the following:

$$\begin{aligned}\max_{(x_i,t_k)\in Q^{M,N}}\left|U_i^k - u(x_i,t_k)\right| &\le C\frac{1}{b_{\alpha\delta}}\max_{1\le k\le N}\left\|\widetilde{R}_i^k + R_i^k\right\|_\infty \\ &\le C\frac{1}{b_{\alpha\delta}}(h^2 + N^{-(1+\alpha)}) \\ &\le C(h^2 + N^{-(1+\alpha)}),\end{aligned}$$

which completes the proof.

6. Numerical experiments

We consider problem (1.1) in the unit interval $[0, 1] \times [0, 1]$ and test it numerically for the following initial data with weak singularities around zero [23]:

$$g(x, t) = (x - x^2)^2 E_{\alpha,1}(|t|^\alpha), \tag{6.1}$$

where the Mittag-Leffler function is defined as $E_{\alpha,\beta}(z) = \sum_{k=0}^{\infty} \frac{z^k}{\Gamma(\alpha k+\beta)}$, and $f \equiv 0$.

Since the analytic solution of this test problem is unknown, we use the mesh approximation with the densest mesh as the exact solution. The maximum errors and the corresponding convergence rates are computed by the following:

$$E^{M,N} := \max_{0\le i\le M} \max_{0\le k\le N} \left| U_i^k - \bar{U}(x_i, t_k) \right|,$$
$$R^{M,N} := \log_2 \left(\frac{E^{M,N}}{E^{2M,2N}} \right),$$

where $U_i^k, k = 0, 1, \cdots, N, i = 0, 1, \cdots, M$, is the numerical solution of $u(x, t)$ at the grid points $Q^{M,N}$, and $\bar{U}(x, t)$ is the piecewise linear interpolation function through points (x_i, t_k, U_i^k), where $i = 0, 1, \cdots, 2048$, and $k = 0, 1, \cdots, 2048$. In the following calculation, we choose the mesh parameter $K = 0.2$.

For $N = M = 2^k, k = 5, 6, \cdots, 11$, $\alpha = 0.3, 0.5, 0.8$, and $\delta = 0.5$, the maximum errors and their corresponding orders of convergence are given in Tables 1–3. The numerical experiments confirm that the optimal convergence order is attained for both the modified graded mesh (MG-mesh) (with parameter $K \in (0, 1)$) and the graded mesh (G-mesh) with $r \ge \frac{1+\alpha}{\alpha}$, which is in complete agreement with the theoretical prediction established in Theorem 5.1. For varying values of α, the numerical solutions of this test problem are displayed in Figure 1 with $N = M = 64$. Meanwhile, the numerical solutions for $u(1/2, t)$ when $\alpha = 0.1, 0.3, 0.5$, and 0.7 are plotted in Figure 2. This figure clearly indicates the presence of an initial layer at $t = 0$, which becomes more pronounced as $\alpha \to 0$.

Table 1. Numerical results by using different meshes with $\alpha = 0.3$ and $T = 1$.

Grid	Parameter	$N = 32$	$N = 64$	$N = 128$	$N = 256$	$N = 512$	$N = 1024$
MG-mesh	$K = 0.2$	6.410E-03	2.706E-03	1.012E-03	4.173E-04	1.651E-04	6.564E-05
		–	1.244	1.419	1.278	1.337	1.331
G-mesh	$r = \frac{2}{\alpha}$	9.334E-03	3.971E-03	1.623E-03	6.134E-04	2.588E-04	1.073E-04
		–	1.233	1.291	1.404	1.245	1.270
	$r = \frac{1+\alpha}{\alpha}$	5.731E-03	2.413E-03	9.566E-04	3.751E-04	1.429E-04	5.613E-05
		–	1.248	1.335	1.351	1.392	1.348
Uniform-mesh		4.447E-03	2.917E-03	1.831E-03	1.087E-03	5.817E-04	2.369E-04
		–	0.608	0.672	0.752	0.903	1.296

A perusal of Tables 1–3 reveals that the numerical outcomes remain largely indistinguishable, regardless of whether the MG-mesh or the graded mesh with $r \ge \frac{1+\alpha}{\alpha}$ is employed for $T = 1$. Therefore, to demonstrate the superiority of the numerical method we proposed, we plot of the maximum error's evolution over time T, considering $\alpha = 0.1, 0.5$ and $N = M = 256$, as shown in

Figure 3. Obviously, with the increment of time T, the error that results from the MG-mesh is markedly lower compared to the error from the G-mesh. In particular, when α takes a smaller value, the advantages of the MG-mesh method are more evident.

Table 2. Numerical results by using different meshes with $\alpha = 0.5$ and $T = 1$.

Grid	Parameter	$N = 32$	$N = 64$	$N = 128$	$N = 256$	$N = 512$	$N = 1024$
MG-mesh	$K = 0.2$	2.242E-03	9.904E-04	4.037E-04	1.457E-04	5.177E-05	1.795E-05
		–	1.179	1.295	1.471	1.492	1.528
G-mesh	$r = \frac{2}{\alpha}$	4.397E-03	2.126E-03	9.543E-04	4.025E-04	1.495E-04	5.273E-05
		–	1.049	1.156	1.245	1.429	1.504
	$r = \frac{1+\alpha}{\alpha}$	3.217E-03	1.496E-03	6.773E-04	2.933E-04	1.050E-04	3.682E-05
		–	1.104	1.143	1.208	1.482	1.512
Uniform-mesh		1.974E-03	1.299E-03	8.122E-04	4.784E-04	2.532E-04	1.219E-04
		–	0.603	0.678	0.764	0.918	1.055

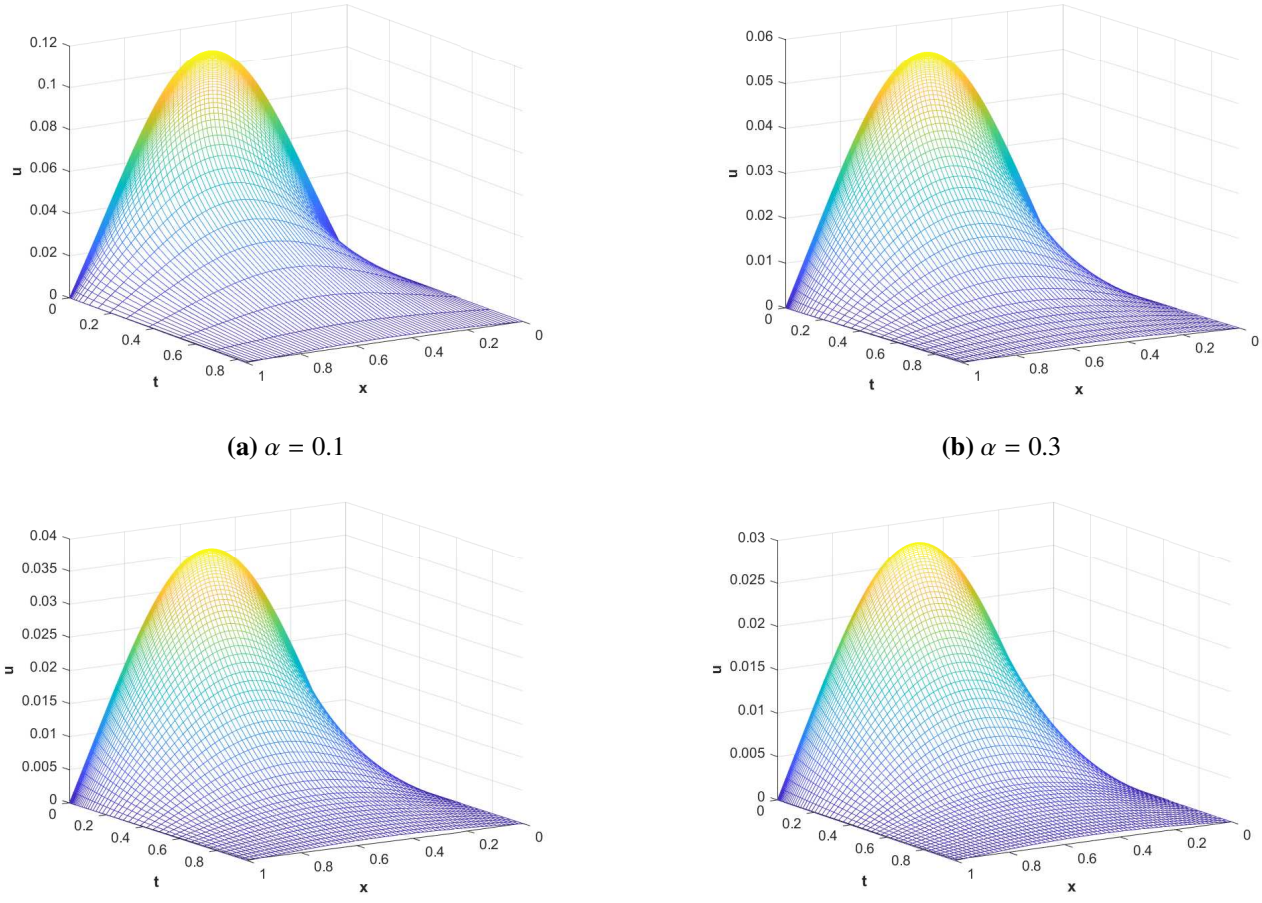

(a) $\alpha = 0.1$ **(b)** $\alpha = 0.3$

(c) $\alpha = 0.5$ **(d)** $\alpha = 0.7$

Figure 1. Numerical solutions with $N = M = 64$ and different values of α.

Table 3. Numerical results by using different meshes with $\alpha = 0.8$ and $T = 1$.

Grid	Parameter	$N = 32$	$N = 64$	$N = 128$	$N = 256$	$N = 512$	$N = 1024$
MG-mesh	$K = 0.2$	1.216E-03	5.936E-04	2.549E-04	1.018E-04	3.400E-05	9.833E-06
		–	1.034	1.220	1.324	1.582	1.790
G-mesh	$r = \frac{2}{\alpha}$	2.534E-03	1.257E-03	5.968E-04	2.771E-04	1.132E-04	3.332E-05
		–	1.011	1.075	1.107	1.292	1.764
	$r = \frac{1+\alpha}{\alpha}$	2.266E-03	1.114E-03	5.787E-04	2.501E-04	1.067E-04	3.244E-05
		–	1.024	1.051	1.105	1.228	1.718
Uniform-mesh		1.106E-03	5.421E-04	2.621E-04	1.388E-04	7.007E-05	3.174E-05
		–	1.028	1.048	0.918	0.986	1.142

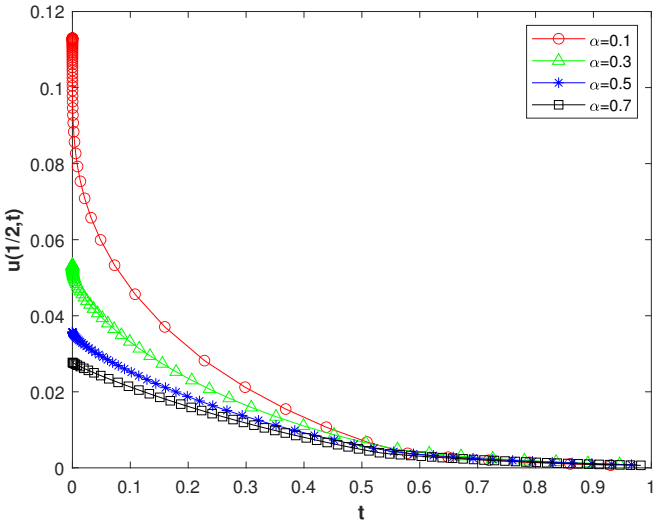

Figure 2. Numerical solutions with $N = M = 64$ and different values of α at $x = 1/2$.

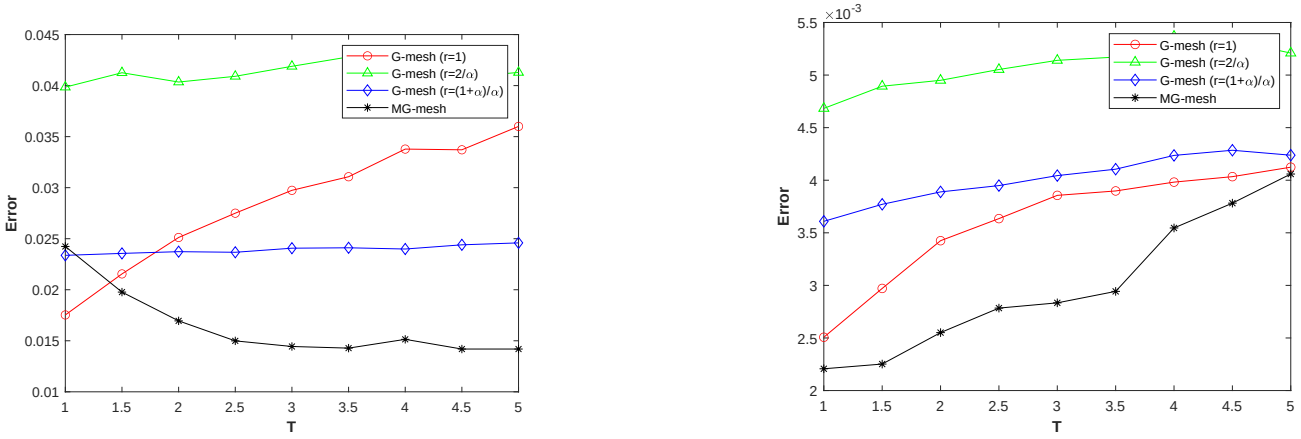

(a) $\alpha = 0.1$ **(b)** $\alpha = 0.5$

Figure 3. Errors as a function of T for MG-mesh and G-mesh with $N = M = 256$ and different values of α.

7. Conclusions

In this article, based on the discussion in references [1, 18, 22], we successfully expand the quadrature-based finite difference method from a uniform grid to a modified graded grid. The numerical experiments showed that the error converged at a rate of $1 + \alpha$. Some properties of the modified grid were discussed, and the convergence results and error estimates of the scheme were given. Both the theoretical and numerical experimental results showed that the modified mesh had the same order of convergence as the graded mesh; additionally, the numerical experiments showed that the modified mesh had a smaller error.

In the study of the discretization of nonlocal-in-time operators, this is the first time that the finite difference method has been successfully applied on a modified graded mesh for a nonlocal time diffusion equation. Its application to other equations with nonlocal-in-time operators will be studied in a further article.

Author contributions

S. L.: conception, validation, formal analyses, data compilation, writing-original manuscript, writing-review, editing, revision, and reorganization; L. L.: methods, supervision, validation, and project management; X. B.: supervision and validation. All authors have read and agreed to the published version of the manuscript.

Use of AI tools declaration

The authors declare they have not used Artificial Intelligence (AI) tools in the creation of this article.

Acknowledgement

This research was funded by the Guangxi Science and Technology Base and Special Talents grand number (Guike AD23023003), Guangxi Natural Science Foundation (2025GXNSFAA069738), the National Natural Science Foundation of China (12361087), the innovation Project of Guangxi Graduate Education (JGY2024267, YCSW2025526) and the Key Program of the Natural Science Foundation of Anhui Province (2024AH051364).

Conflict of interest

The authors declare there is no conflict of interest.

References

1. Q. Du, J. Yang, Z. Zhou, Analysis of a nonlocal-in-time parabolic equation, *Discrete Contin. Dyn. Syst. B*, **22** (2017), 339–368. http://dx.doi.org/10.3934/DCDSB.2017016
2. K. Huang, Q. Du, Asymptotic compatibility of a class of numerical schemes for a nonlocal traffic flow model, *SIAM J. Numer. Anal.*, **62** (2024), 1119–1144. http://dx.doi.org/10.1137/23M154488X

3. F. Bobaru, M. Duangpanya, The peridynamic formulation for transient heat conduction, *Int. J. Heat Mass Transfer*, **53** (2010), 4047–4059. https://doi.org/10.1016/j.ijheatmasstransfer.2010.05.024

4. L. Feo, G. Lovisi, R. Penna, Free vibration analysis of functionally graded nanobeams based on surface stress-driven nonlocal model, *Mech. Adv. Mater. Struct.*, **31** (2024), 10391–10399. https://doi.org/10.1080/15376494.2023.2289079

5. V. Sidorov, E. Badina, R. Tsarev, Dynamic model of beam deformation with consider nonlocal in time elastic properties of the material, *Int. J. Comput. Civ. Struct. Eng.*, **18** (2022), 124–131. https://doi.org/10.22337/2587-9618-2022-18-4-124-131

6. Z. F. Weng, X. Q. Yue, S. Y. Zhai, A second order accurate SAV numerical method for the nonlocal ternary conservative Allen-Cahn model, *Appl. Math. Lett.*, **142** (2023), 108633. https://doi.org/10.1016/j.aml.2023.108633

7. S. Pal, R. Melnik, Nonlocal models in biology and life sciences: Sources, developments, and applications, *Phys. Life Rev.*, **53** (2025), 24–75. https://doi.org/10.1016/j.plrev.2025.02.005

8. Z. F. Weng, S. Y. Zhai, X. L. Feng, Numerical approximation of the nonlocal ternary viscous Cahn-Hilliard model based on a high order explicit hybrid algorithm, *SIAM J. Sci. Comput.*, **47** (2025), A2221–A2247. https://doi.org/10.1137/24M1645474

9. X. D. Zhang, L. L. Wei, J. Liu, Application of the LDG method using generalized alternating numerical flux to the fourth-order time-fractional sub-diffusion model, *Appl. Math. Lett.*, **168** (2025), 109580. https://doi.org/10.1016/j.aml.2025.109580

10. Y. L. Feng, X. D. Zhang, Y. Chen, L. Wei, A compact finite difference scheme for solving fractional Black-Scholes option pricing model, *J. Inequal. Appl.*, **2025** (2025), 36. https://doi.org/10.1186/s13660-025-03261-2

11. S. Y. Zhai, Z. F. Weng, Y. F. Yang, A high order operator splitting method based on spectral deferred correction for the nonlocal viscous Cahn-Hilliard equation, *J. Comput. Phys.*, **446** (2021), 110636. https://doi.org/10.1016/j.jcp.2021.110636

12. X. C. Tian, Q. Du, Analysis and comparison of different approximations to nonlocal diffusion and linear peridynamic equations, *SIAM J. Numer. Anal.*, **51** (2013), 3458–3482. https://doi.org/10.1137/13091631X

13. D. Mezzanotte, D. Occorsio, E. Venturino, Analysis of a line method for reaction-diffusion models of nonlocal type, *Appl. Numer. Math.*, **203** (2024), 255–268. https://dx.doi.org/10.1016/j.apnum.2024.05.011

14. L. L. Li, Y. Y. Fu, Unconditional error estimate of linearly-implicit and energy-preserving schemes for nonlocal wave equations, *Comput. Math. Appl.*, **176** (2024), 492–509. https://doi.org/10.1016/j.camwa.2024.11.002

15. H. Tian, J. K. Lu, L. L. Ju, A novel bond-based nonlocal diffusion model with matrix-valued coefficients in non-divergence form and its collocation discretization, *Comput. Math. Appl.*, **173** (2024), 33–46. https://doi.org/10.1016/j.camwa.2024.08.002

16. J. S. Lu, L. Zhang, X. C. Guo, Q. Qi, A POD based reduced-order local RBF collocation approach for time-dependent nonlocal diffusion problems, *Appl. Math. Lett.*, **160** (2025), 109328. https://doi.org/10.1016/j.aml.2024.109328
17. Z. F. Weng, S. Y. Zhai, W. Z. Dai, Y. Yang, Y. Mo, Stability and error estimates of Strang splitting method for the nonlocal ternary conservative Allen-Cahn model, *J. Comput. Appl. Math.*, **441** (2024), 115668. https://doi.org/10.1016/j.cam.2023.115668
18. A. Chen, Q. Du, C. P. Li, Z. Zhou, Asymptotically compatible schemes for space-time nonlocal diffusion equations, *Chaos, Solitons Fractals*, **102** (2017), 361–371. https://doi.org/10.1016/j.chaos.2017.03.061
19. J. Kemppainen, R. Zacher, Long-time behavior of non-local in time Fokker–Planck equations via the entropy method, *Math. Models Methods Appl. Sci.*, **29** (2019), 209–235. https://doi.org/10.1142/S0218202519500076
20. Q. Du, Z. Zhou, Nonlocal-in-time dynamics and crossover of diffusive regimes, *Int. J. Numer. Anal. Model.*, **20** (2023), 353–370. https://doi.org/10.4208/ijnam2023-1014
21. V. Sidorov, M. Shitikova, E. Badina, E. Detina, Review of nonlocal-in-time damping models in the dynamics of structures, *Axioms*, **12** (2023), 676. https://doi.org/10.3390/axioms12070676
22. L. B. Liu, L. Xu, Y. Zhang, Error analysis of a finite difference scheme on a modified graded mesh for a time-fractional diffusion equation, *Math. Comput. Simul.*, **209** (2023), 87–101. https://doi.org/10.1016/j.matcom.2023.02.007
23. C. P. Li, Q. Yi, A. Chen, Finite difference methods with non-uniform meshes for nonlinear fractional differential equations, *J. Comput. Phys.*, **316** (2016), 614–631. https://doi.org/10.1016/j.jcp.2016.04.039

AIMS Press